Identification of Histidine As an Axial Ligand to P_{700}^{+} †

Michelle Mac,‡ Xiao-Song Tang,§ Bruce A. Diner,§ John McCracken,‡ and Gerald T. Babcock*,‡

Department of Chemistry, Michigan State University, East Lansing, Michigan 48824, and Central Research and Development Department, Experimental Station, E. I. DuPont de Nemours and Company, Wilmington, Delaware 19880

Received July 18, 1996; Revised Manuscript Received September 3, 1996⊗

ABSTRACT: The primary electron donor in photosystem I (PSI), P_{700}, is thought to be a dimeric Chl *a* species. Neither the electronic nor geometric structure of the cation radical is clearly understood. Magnetic resonance studies have indicated that the unpaired electron in P_{700}^{+} is delocalized asymmetrically over the Chl *a* dimer; however, the axial ligand to the central Mg^{2+} is not known. The recent development of a histidine tolerant mutant of *Synechocystis* PCC 6803 has allowed us to use a combination of isotopic labeling and electron nuclear double resonance (ENDOR) spectroscopy to show the first definitive spectroscopic evidence of a histidine ligand to P_{700}^{+}. Peaks split symmetrically about the ^{15}N Larmor frequency corresponding to an isotropic hyperfine coupling of 0.64 MHz were observed in the ENDOR spectra from P_{700}^{+} globally labeled with ^{15}N and specifically labeled with [^{15}N]histidine. These peaks disappeared in "reverse" labeled samples in which all nitrogens are ^{15}N except those of histidine, which contains natural abundance ^{14}N. The dipolar contribution to the hyperfine coupling was determined by using electron spin echo envelope modulation spectroscopy (ESEEM). Numerical simulations of the ESEEM data suggest that the coupling is primarily isotropic and that the histidine is directly coordinated to the central Mg^{2+} of P_{700}^{+} . Taken together, these data are supportive of a model of P_{700}^{+} in which the excited state molecular orbital makes a significant contribution to the electronic structure of the radical. Moreover, the methodology developed in this work can be extended to examine the magnetic properties of axial ligands in a variety of biologically relevant porphyrin/chlorin systems.

Oxygenic photosynthesis in higher plants and cyanobacteria requires the interplay of two pigment−protein reaction centers, photosystem I and photosystem II (PSI and PSII). PSI mediates the production of oxidized plastocyanin and reduced nicotinamide adenine dinucleotide phosphate (NADPH), which is used by the plant to fuel the enzymatic cycles associated with the assimilation of carbon dioxide [for review see Golbeck (1992)]. PSII is associated with water oxidation and is the site of oxygen evolution [for reviews see Diner and Babcock (1996) and Britt (1996)]. In each of these reaction centers, light-induced electron transfer from a chlorophyll *a* species (P_{700} in PSI and P_{680} in PSII) to a series of cofactors that serve as sequential electron acceptors results in a charge separation process with a quantum yield that approaches unity.

Although significant progress has been made in solving the crystal structure of PSI (Krauss *et al.*, 1993; Fromme *et al.*, 1996), the resolution is not yet sufficient to provide a clear view of the geometric structure of P_{700}^{+}; neither the nuclearity nor the ligation sphere of the species has been determined. However, for bacterial reaction centers, X-ray crystallographic studies have shown that the primary donor consists of a dimer of BChl[1] with each BChl having a single histidine ligand (Deisenhofer *et al.*, 1985; Allen *et al.*, 1987). Recent chemically induced dynamic nuclear polarization experiments have confirmed the presence of this nitrogen based ligand (Zysmilich & McDermott, 1994). Specific mutation of either of these ligands to leucine or phenylalanine (Schenck *et al.*, 1990) results in the loss of Mg^{2+} from the associated BChl and the generation of a BChl/BPheo heterodimer (Bylina & Youvan, 1988). Interestingly, the replacement of histidine with glycine does *not* result in the replacement of BChl with BPheo; a coordinating water molecule is thought to stabilize the P^{+} structure (Goldsmith *et al.*, 1996).

EPR spectroscopy is an invaluable tool for studying the geometric and electronic structure of P_{700}^{+} in PSI because elucidation of the electron-nuclear hyperfine coupling constants for a radical will provide a direct measurement of its highest occupied molecular orbital. However, because the EPR signal from P_{700}^{+} consists of a single resonance line (Commoner *et al.*, 1956) that is inhomogeneously broadened by the presence of multiple overlapping hyperfine interactions, information regarding the magnitude of these hyperfine coupling constants is obscured. These couplings can be resolved by the application of advanced EPR techniques. ^{1}H and ^{15}N ENDOR and electron spin echo envelope modulation (ESEEM) studies on frozen solutions of PSI have indicated (Davis *et al.*, 1993; Käss *et al.*, 1995; Käss & Lubitz, 1996) that P_{700}^{+} is a dimeric Chl *a* species characterized by an asymmetrical spin density distribution similar to that found in the bacterial reaction centers (Lendzian *et al.*, 1988, 1993).

The identity of the axial ligand(s) to P_{700}^{+} remains uncertain as previous attempts at identification by using a

† This work was supported by the National Institutes of Health Grants GM-54065 (J.M.) and GM-37300 (G.T.B.) and the USDA CRGO Photosynthesis Program (G.T.B.). B.A.D. gratefully acknowledges support from the NRI/CRGP of the USDA. EPR instrumentation was purchased, in part, with funds supplied by the NIH through Grant Number RR10381 (J.M. and G.T.B.).

* Author to whom correspondence should be addressed.

‡ Michigan State University.

§ E. I. DuPont de Nemours and Company.

⊗ Abstract published in *Advance ACS Abstracts,* October 1, 1996.

[1] Abbreviations: BChl, bacteriochlorophyll; BPheo, bacteriopheophytin; Chl, chlorophyll; ENDOR, electron nuclear double resonance; ESEEM, electron spin echo envelope modulation.

S0006-2960(96)01765-5 CCC: $12.00

combination of biochemical manipulation and subsequent spectroscopic evaluation have been inconclusive (Cui *et al.*, 1995). The presence of histidine ligands to P^+ in the bacterial reaction centers, as well as conserved histidine residues in the amino acid sequence of psaB, the PSI protein known to bind P_{700}, suggests this residue as the most likely candidate (Robert & Moenne-Loccoz, 1990; Golbeck, 1992). Recent proton ENDOR and ESEEM experiments on mutants of *Chlamydomas reinhardtii* indicate that the observed spectroscopic properties of the primary donor in this system are not affected by mutations of his523, a highly conserved residue that is a good candidate for the putative histidine ligand to P_{700}^+ (Cui *et al.*, 1995). These mutations were expected to replace a Chl *a* with a pheophytin, analogous to the bacterial system; however, the ENDOR and ESEEM spectra collected on these mutants (H523Q and H523L) failed to detect any changes in the unpaired electron spin distribution for the radical. Because the spin density distribution for a pheophytin molecule differs considerably from that of chlorophyll (Plato *et al.*, 1990), it was concluded that H523 is not a ligand to P_{700}^+. The possibility that the induced mutations could have allowed water access to the binding site as a bridging ligand (Goldsmith *et al.*, 1996), preserving the integrity of the P_{700}^+ structure, could not be ruled out. Moreover, since the X-band ESEEM spectrum is dominated by contributions from the pyrrole nitrogen atoms of the Chl a macrocycle, perturbations in the hyperfine coupling resulting from changes to the axial ligand would be difficult to detect.

The recent development of histidine-tolerant mutants (Tang *et al.*, 1994a) of the cyanobacterium *Synechocystis* PCC 6803 has allowed for specific isotopic labeling of the histidine nitrogens. By using a combination of ENDOR and ESEEM spectroscopies and these specifically labeled samples, we are able to present the first definitive spectroscopic evidence for a histidine ligand to P_{700}^+.

MATERIALS AND METHODS

Strains and Cell Growth. A histidine-tolerant strain was isolated from the cyanobacterium *Synechocystis* PCC 6803 as described previously (Tang *et al.*, 1994a). Cells of this strain were grown photoautotrophically at 30 °C for 5 days in 10-L carboys by using cool-white fluorescent lamps (7 W/m^2). BG-11 medium (Rippke *et al.*, 1979) was supplemented with 240 μM of either DL-histidine containing only natural-abundance ^{14}N or DL-histidine containing two ^{15}N atoms in its imidazole group. For ^{15}N global labeling, 99.9% [^{15}N]nitrate was used as the sole nitrogen source during cell growth. For [^{14}N]histidine-reverse labeling, this [^{15}N]nitrate containing BG-11 medium was supplemented with 240 μM [^{14}N]histidine. The growth medium was bubbled with 5% CO_2 in air. With these experimental conditions, approximately 85% of the histidine molecules incorporated into thylakoid proteins were from the histidine supplemented in the growth medium as shown previously by mass analysis of histidine (Tang *et al.*, 1994a).

Preparation of PSI Core Complexes. PSI core complexes were purified according to the procedure described earlier (Tang & Diner, 1994b). The complexes were eluted from DEAE-Toyopearl 650s column by using 50 mM $MgSO_4$ in 50 mM MES-NaOH buffer (pH = 6.0) containing 0.03% dodecyl maltoside, 25% (w/v) glycerol, 5 mM $MgCl_2$, and 20 mM $CaCl_2$. The samples were desalted by passage through a gel filtration column (Econo-Pac 10DG, Bio-Rad) equilibrated with 50 mM HEPES-NaOH (pH = 7.5) buffer containing 10 mM NaCl and 0.03% dodecyl maltoside and then concentrated down to about 15 mg of chl/mL by using centricon 100 (Amicon). To generate P_{700}^+, 1 mM potassium ferricyanide was added to the samples. Finally, the samples were loaded into 4 mm OD EPR tubes and frozen in liquid nitrogen.

ENDOR Spectroscopy and Data Analysis. The ENDOR data were obtained at X-band on a Bruker ESP300e spectrometer with a Bruker ESP360 DS ENDOR accessory and home-built demountable coils (Bender *et al.*, 1989). All ENDOR data were collected at a field position corresponding to the center of the EPR absorption line. Constant temperature in the cavity was maintained with an Oxford ESR900 continuous flow cryostat. Microwave frequency was determined by using an EIP Microwave model 25B frequency counter, and the static magnetic field strength was measured with a Bruker ER035M NMR gaussmeter.

The peaks attributed to ^{15}N ($I = {}^1/_2$) electron nuclear hyperfine coupling are expected to be split symmetrically about the nuclear Larmor frequency for ^{15}N ($\nu^{15}_N = 1.45$ MHz at 3500 G). In solution ENDOR, the position of these peaks is indicative of the strength of the isotropic hyperfine coupling according to the relationship (Kevan & Kispert, 1976)

$$\nu_\pm = \nu_N \pm A_{iso}/2$$

where $\nu_N \geq A_{iso}/2$. However, in frozen solution, the anisotropy of the hyperfine coupling gives rise to powder line shapes described to first order by

$$\nu_\pm = \nu_N \pm A/2$$

where

$$A = A_{||} \cos^2 \theta + A_\perp \sin^2 \theta.$$

$A_{||}$ and $A_\perp$ in the above expression are the principal values of the axially symmetric hyperfine tensor, and θ describes the orientation of the principal axis system of the hyperfine tensor with respect to the laboratory magnetic field (Blinder, 1960).

ESEEM Data Collection and Analysis. ESEEM data were collected on a home-built spectrometer (McCracken *et al.*, 1992) by using a reflection cavity where either folded stripline (Lin *et al.*, 1985) or slotted-tube structures (Mehring & Freysoldt, 1980) served as the resonant element. A three-pulse or stimulated echo (90°-τ-90°-T-90°) pulse sequence was used. Dead time reconstruction was performed prior to Fourier transformation as described (Mims, 1984). Computer simulations of the ESEEM data were performed on a Sun Sparcstation 2 computer utilizing FORTRAN software based on the density matrix formalism of Mims (1972). The analysis software for the treatment of experimental and simulated ESEEM data was written with Matlab (Mathworks, Nantick, MA). The experimental dead time was included in the simulations. An isotropic **g**-tensor was assumed in all of the calculations. The success of the spectral simulations was based on the modulation depth and duration observed in the time domain traces as well as the line shapes, peak positions, and relative peak intensities in the frequency spectra.

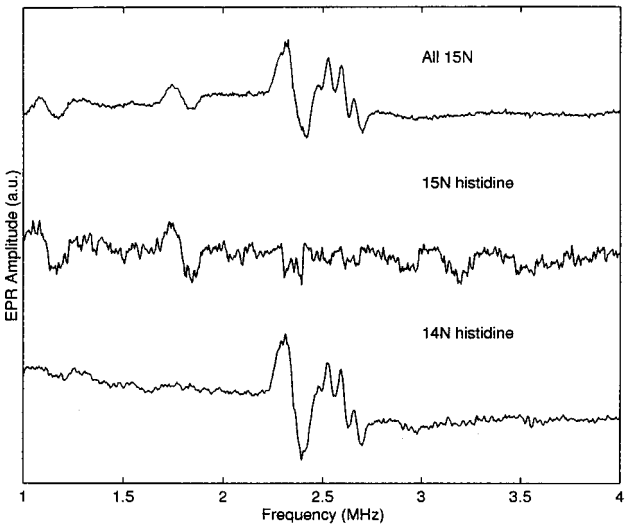

FIGURE 1: ENDOR spectra collected at 6 K for P_{700}^+ globally labeled with ^{15}N (top), specifically labeled with [^{15}N]histidine (middle), and "reverse" labeled [^{14}N]histidine in the presence of [^{15}N]nitrate (bottom). Spectrometer conditions for all spectra, unless otherwise indicated: microwave power, 1.99 mW; magnetic field strength, 3375 G (top), 3356 G (middle), 3367 G (bottom); RF power, 200 W; RF frequency modulation, 100 kHz.

RESULTS

The use of ENDOR spectroscopy in conjunction with ESEEM in these studies exhibits the complementarity of the two techniques. Couplings containing a large dipolar component are usually difficult to detect with ENDOR, since the broadened powder pattern line shape precludes resolution of the turning points. In contrast, the dipolar portion of the hyperfine coupling mixes the nuclear states within each electron spin manifold and enables the "forbidden" EPR transitions that give rise to ESEEM. Similarly, purely isotropic hyperfine couplings will result in discrete EPR transitions from each hyperfine level and eliminate the interference effects that give rise to the modulations (Mims, 1972). ENDOR spectroscopy can, therefore, be used to resolve primarily isotropic nitrogen couplings, while ESEEM is suited best for hyperfine couplings that contain a considerable dipolar contribution. The degree of this contribution can be quantitated by applying both techniques.

The ENDOR first-derivative spectrum collected at 6 K for P_{700}^+ globally labeled with ^{15}N is shown in Figure 1 (top). The analogous spectra from P_{700}^+ specifically labeled with ^{15}N-histidine and "reverse" labeled so that all nitrogens are ^{15}N except those of histidine, which contains natural abundance ^{14}N, are shown in Figure 1, middle and bottom, respectively. Features observed in the spectra of Figure 1 are expected to arise from all ^{15}N nuclei coupled to the electron spin; these include nitrogens in the chlorophyll macrocycle as well as in the putative histidine ligand. By using specific isotope labeling, identification of the peaks arising from this ligand is facilitated. The peaks at 1.13 and 1.78 MHz appear in the spectrum from the globally labeled sample (Figure 1, top) as well as in the spectrum from P_{700}^+ containing ^{15}N-labeled histidine (Figure 1, middle). Upon reverse labeling, these peaks disappear (Figure 1, bottom), thus confirming histidine as their origin. These features are split symmetrically about the Larmor frequency for ^{15}N and correspond to an isotropic hyperfine coupling of 0.64 MHz. Moreover, features in the 2−3 MHz region can be assigned

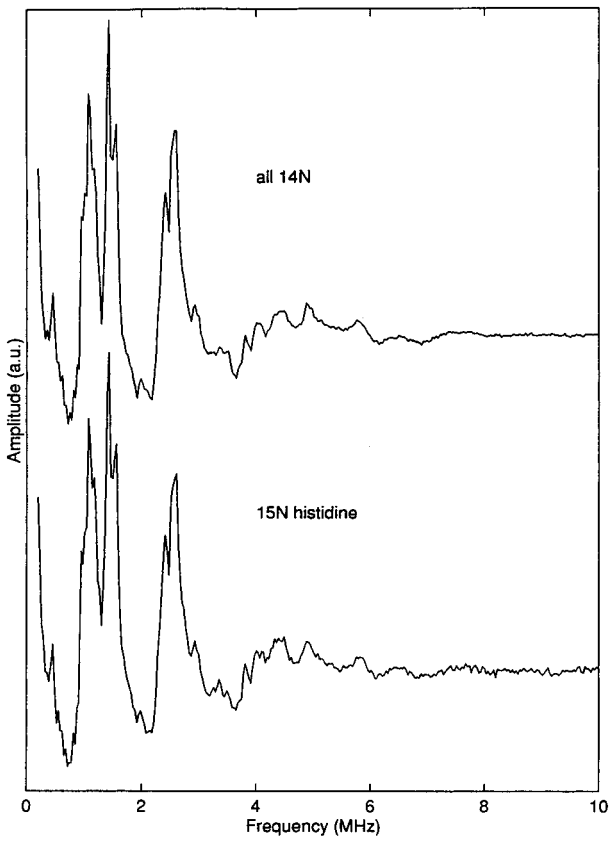

FIGURE 2: Fourier transformations of three-pulse ESEEM data from P_{700}^+ containing natural abundance ^{14}N (top) and specifically labeled with [^{15}N]histidine (bottom). Spectrometer conditions: magnetic field strength, 3210 G (top), 3195 G (bottom), microwave pulse power, 45 dBm; microwave pulse length (FWHM), 15 ns; pulse repetition rate, 20 Hz; τ value, 175 ns; sample temperature, 4 K.

definitively to contributions from the nitrogens in the chlorophyll *a* macrocycle. A comprehensive analysis of these chlorophyll pyrrole nitrogen couplings by using multifrequency ESEEM and ^{15}N ENDOR is currently in progress.

The presence of this nitrogen derived histidine coupling does not affect the ESEEM spectrum as demonstrated in Figures 2 and 3. The cosine Fourier transformation of three-pulse time domain data from P_{700}^+ containing natural abundance ^{14}N is identical (Figure 2, top) to the spectrum from P_{700}^+ specifically labeled with [^{15}N]histidine (Figure 2, bottom). These spectra are dominated by ^{14}N modulations from the Chl *a* pyrrole nitrogens and are typical for situations where the hyperfine interaction is approximately equal to twice the nuclear Zeeman energy. Under these conditions the energy level splittings in the spin manifold where the nuclear Zeeman and electron−nuclear hyperfine interactions cancel are determined primarily by the ^{14}N nuclear quadrupole interaction. This exact cancellation condition is characterized by modulations that are deep and long-lived. Because these modulations will dominate the ESEEM spectrum, contributions from the nitrogen of the histidine ligand, which is away from exact cancellation, are not expected to be observed. To eliminate this deep ^{14}N ESEEM from our measurements, analogous three-pulse ESEEM experiments were performed on the ^{15}N enriched and

[2] Multifrequency ESEEM and analysis of the field dependence of the frequencies indicate that the minor components near 1 and 2.3 MHz are due to residual ^{14}N. The presence of this residual ^{14}N was confirmed with mass spectrometry.

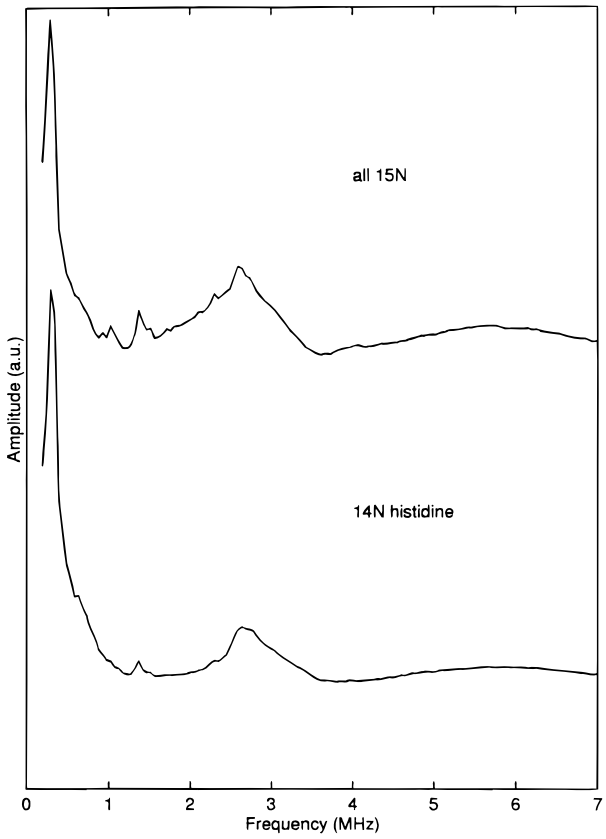

FIGURE 3: Three-pulse ESEEM frequency spectra from P_{700}^+ globally enriched with ^{15}N (top) and "reverse" labeled (bottom). Spectrometer conditions: magnetic field strength, 3195 G; microwave pulse power, 45 dBm; microwave pulse length (FWHM), 15 ns; pulse repetition rate, 90 Hz; τ value, 250 ns; sample temperature, 4 K.

"reverse" labeled samples (Figure 3, top and bottom, respectively). No differences were resolved in the spectra, indicating a minimal contribution to the ESEEM spectra from nitrogen hyperfine coupling originating from the histidine.[2]

DISCUSSION

The presence of a histidine ligand bound to the central Mg^{2+} atom of P_{700}^+ has often been postulated as it has been shown to ligate the primary donor in the bacterial reaction center (Allen *et al.*, 1987; Deisenhofer *et al.*, 1985; El-Kabbani *et al.*, 1991) but until now has not been demonstrated unambiguously. Spectroscopic characterization of this ligand is necessary to understand the optical and magnetic properties of the cation radical. Modulation of these properties is thought to occur by interactions of the chromophore with its protein environment through, for example, hydrogen bond interactions with nearby amino acid residues or through axial ligation to the Mg^{2+}. In heme proteins, cavity mutants generated by site directed mutagenesis allow the introduction of exogeneous organic ligands that greatly affect the functional properties of the protein (DePillis *et al.*, 1994). A similar strategy to examine the effect of axial ligands on magnetic and optical properties of the primary donor of bacterial reaction centers has been applied by Goldsmith *et al.* (1996). However the lack of an adequate spectroscopic probe has precluded characterization of the ligand. Identification of a histidine ligand to P_{700}^+ provides the spectroscopic methodology necessary for characterization of these mutants.

It is possible, however, that the histidine-derived nitrogen hyperfine coupling shown in Figure 1 arises from a histidine residue hydrogen bonded to the 9-keto group of the conjugated π-system of the chlorophyll *a*. Amino acid residues interacting non-covalently with the primary electron donors in photosynthetic reaction centers from a variety of organisms have been suggested as the source of the disparity in their redox potentials and optical properties (Lin *et al.*, 1994). The role of H-bonded residues as redox potential "tuning modules" is not unusual in biological systems; it has been suggested as an explanation for the wide range of redox potentials observed for [*n*Fe-*m*S] clusters (Backes *et al.*, 1991) and has recently been shown to alter the internal charge transfer state in BChl−BPheo heterodimer mutants in bacterial reaction centers (Allen *et al.*, 1996). The precedence of histidine residues in H-bonded interactions with P^+ has been demonstrated in the bacterial reaction centers (Rautter *et al.*, 1995). Although the H-bonded histidine was not detected directly by spectroscopic methods, changes in the redox potential and unpaired electron spin density distribution subsequent to mutations of his L168 led to conclusions that this residue participates in a hydrogen bond with the 2-acetyl group of the BChl. However, because the spin density distribution of P^+ in bacterial reaction centers differs from that of P_{700}^+ in PSI (Davis *et al.*, 1993; Käss *et al.*, 1995; Käss & Lubitz, 1996), the lack of spectroscopic evidence for this H-bonded histidine does not preclude detection in PSI. Therefore, even without a covalent interaction, ENDOR spectroscopy could detect the coupling from a H-bonded moiety provided that sufficient dipolar coupling between the unpaired π-electron of the radical and the nitrogen nucleus are present.

Hydrogen-bonding interactions of this genre have been studied in other paramagnetic systems, both *in vivo* and *in vitro*, and can provide information regarding the form of the hyperfine tensors expected. In powder samples, these interactions were characterized initially by O'Malley and Babcock (1986) who used isotopic labeling and ENDOR spectroscopy to investigate H-bonds in *p*-benzoquinone anion radicals. The proton hyperfine coupling tensor for solvent protons H-bonded to the oxygen of the semiquinone radical in this system was shown to be axially symmetric. The ratio of −1:−1:2 for the principal values was determined and corroborated by earlier results from single-crystal work (Reddy *et al.*, 1982). *In vivo*, these interactions have been studied extensively in a variety of systems containing Fe-S centers. The hyperfine tensors of both the proton and nitrogen involved in the hydrogen bonding interaction have been determined from electron magnetic resonance experiments. Pulsed $^{1,2}H$ ENDOR and $^{2}H-^{2}H$ TRIPLE were used by Doan *et al.* (1994) to determine the intrinsic hyperfine coupling of three strong NH···S hydrogen bonds in the $[Fe_3S_4(cys)_3]^{2-}$ cluster in hydrogenase from *Desulfovibrio gigas*. Surprisingly, the hyperfine tensors for the protons hydrogen bonded to the cysteinyl sulfur contained a substantial isotropic interaction, although no covalent bond exists between the proton and sulfur atoms. Molecular orbital calculations have shown that the unpaired electron spin in these systems is highly centralized on the individual Fe atoms, as much as 80% of the total spin in the case of Fe^{2+}, and most likely contributes to the isotropic character of the proton coupling through a spin polarization or hyperconjugation mechanism (Mouesca *et al.*, 1995). Spin density is

found on the peptide nitrogen nucleus as well and has been observed spectroscopically by Cammack *et al.* (1988) from an Fe-S cluster of fumarate reductase from *Escherichia coli*. In these studies, the hyperfine and quadrupole parameters for a nitrogen atom assigned to an NH···S type hydrogen bond to the cluster were determined by using ESEEM spectroscopy and numerical simulations of the ESEEM data. Observation of the nitrogen coupling was again dependent on the presence of a large amount of unpaired spin density localized on the Fe of the cluster.

It is unlikely that these spectroscopic methods could be used to detect an H-bonded histidine in P_{700}^+. The spin density distribution on the 9-keto oxygen, although not determined definitively, has been estimated to be on the order of 0.4% in the chlorophyll *a* cation radical *in vitro* (Petke *et al.*, 1980). The majority of the unpaired spin in these systems is delocalized on the methine carbon atoms and the four nitrogen atoms (Hanson, 1990). However, if the peaks attributed to the nitrogen of the histidine observed in the ENDOR spectra of Figure 1 (top and middle) *do* represent the perpendicular components of a purely dipolar hyperfine tensor, then the corresponding parallel components would be expected in the 2 MHz region of the spectra. No discernable peaks can be seen in this frequency range in either of the spectra. The resolution of the parallel components of the hyperfine tensor can be difficult as the number of orientations with parallel symmetry contributing to the overall line shape is small, and the lack of these features is not indicative of a purely isotropic hyperfine interaction.

To estimate the dipolar contribution to the observed [^{15}N]-histidine hyperfine coupling, numerical simulations of ESEEM data from ^{15}N-enriched P_{700}^+ were performed. Because the modulation depth observed in an ESEEM experiment relies on the quantum mechanical mixing of the nuclear states that occurs as a result of this contribution, it can be used to determine the dipolar character of a coupling. ^{15}N ESEEM simulations using a purely dipolar tensor, $A_\perp = -0.64$ MHz, $A_\parallel = 1.28$ MHz, predict that a broad feature, centered at the ^{15}N Larmor frequency, 1.4 MHz, would be observed under our experimental conditions (see Figure 4). These simulations indicate that the peaks observed in the ENDOR spectrum are primarily isotropic in character and are consistent with a nitrogen participating in a covalent bond with the Mg^{2+}.

The presence of an isotropic coupling to the nitrogen of the histidine ligand implies a non-zero spin density on the Mg^{2+} atom of P_{700}^+. Molecular orbital calculations on chlorophyll *a* monomers have shown that the availability of a low lying excited state with a decidedly different spin distribution that can influence the electronic structure of the radical and subsequently its magnetic resonance characteristics (Petke *et al.*, 1980). The spin density distribution of this excited state A_{2u} molecular orbital includes spin delocalized on the Mg^{2+} atom (Fajer *et al.*, 1977). ENDOR experiments comparing the magnitude of proton hyperfine couplings in P_{700}^+ to those of chlorophyll *a* model compounds led O'Malley and Babcock (1984) to suggest that the ground state orbital for P_{700}^+ contains 75% ground state and 25% excited state character. These researchers suggested that interactions of P_{700}^+ with its protein environment, either through axial ligation of the Mg^{2+} atom or by electrostatic interactions of the radical with nearby charged amino acid residues, could provide the perturbation necessary to mix

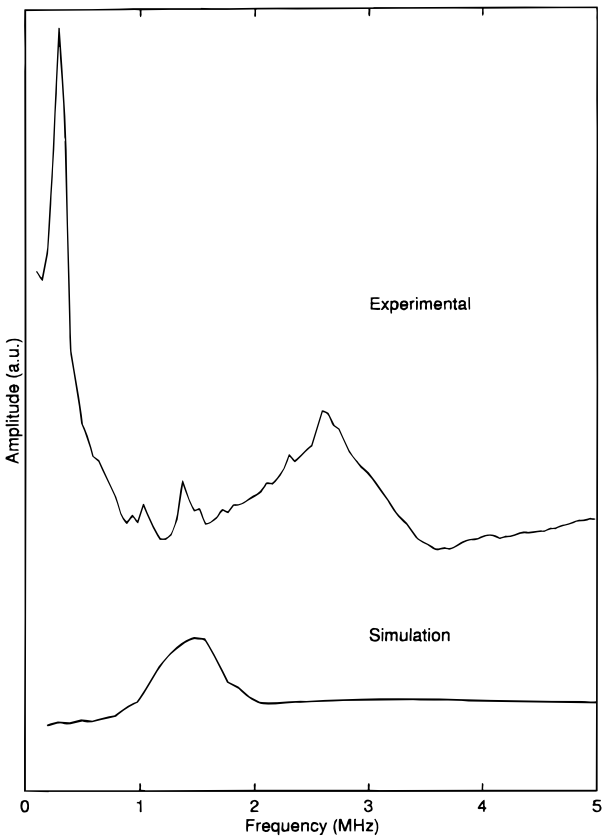

FIGURE 4: Fourier transformation of three-pulse experimental (top) and simulated (bottom) ESEEM spectra from P_{700}^+ globally labeled with ^{15}N. Experimental conditions were identical to those of Figure 3. Simulation parameters: $A_\perp = -0.64$ MHz; $A_\parallel = 1.28$ MHz; all other parameters were identical to those of the experimental spectrum.

the ground and excited state molecular orbitals. These data and the presence of a spectroscopically active histidine ligand to P_{700}^+ exhibiting an isotropic hyperfine interaction are supportive of a model of P_{700}^+ where the excited state orbital makes a significant contribution to the spin density distribution of the cation radical and may explain the differences in redox potentials and optical properties observed for the plant and bacterial primary donor species.

ACKNOWLEDGMENT

^{15}N-labeled histidine was provided by the NIH National Stable Isotope Resource of the Los Alamos National Laboratory. Mass spectral data were obtained at the Michigan State University Mass Spectrometry Facility which is supported, in part, by a grant (DRR-00480) from the Biotechnology Research Technology Program, National Center for Research Resources, National Institutes of Health.

REFERENCES

Allen, J. P., Feher, G., Yeates, T. O., Komiya, H., & Rees, D. C. (1987) *Proc. Natl. Acad. Sci. U.S.A. 84*, 5730−5734.

Allen, J. P., Artz, K., Lin, X., Williams, J. C., Ivancich, A., Albouy, D., Mattioli, T. A., Fetsch, A., Kuhn, M., & Lubitz, W. (1996) *Biochemistry 35*, 6612−6619.

Backes, G., Mino, Y., Loehr, T. M., Meyer, T. E., Cusanovich, M. A., Sweeney, W. V., Adman, E. T., & Sanders-Loehr, J. (1991) *J. Am. Chem. Soc. 113*, 2055−2064.

Bender, C. J., Sahlin, M., Babcock, G. T., Barry, B. A., Chandrashekar, T. K., Salowe, S. P., Stubbe, J., Lindstrom, B., Petersson, L., Ehrenberg, A., & Sjoberg, B.-M. (1989) *J. Am. Chem. Soc. 111*, 8076−8083.

Blinder, S. M. (1960) *J. Chem. Phys 33*, 748−752.
Britt, R. D. (1996) in *Advances in Photosynthesis* (Ort, D., & Yocum, C. F., Eds.) pp 137−164, Kluwer, Dordrecht, The Netherlands.
Bylina, E. J., & Youvan, D. C. (1988) *Proc. Natl. Acad. Sci. U.S.A. 85*, 7226−7230.
Cammack, R., Chapman, A., McCracken, J., Cornelius, J. B., Peisach, J., & Weiner, J. H. (1988) *Biochim. Biophys. Acta 956*, 307−312.
Commoner, B., Heise, J. J., & Townsend, J. (1956) *Proc. Natl. Acad. Sci. U.S.A. 42*, 710−718.
Cui, L., Bingham, S. E., Kuhn, M., Kass, H., Lubitz, W., & Webber, A. N. (1995) *Biochemistry 34*, 1549−1558.
Davis, I. H., Heathcote, P., MacLachlan, D. J., & Evans, M. C. W. (1993) *Biochim. Biophys. Acta 1143*, 183−189.
Deisenhofer, J., Epp, O., Miki, K., Huber, R., & Michel, H. (1985) *Nature 318*, 618−624.
DePillis, G. D., Decatur, S. M., Barrick, D., & Boxer, S. G. (1994) *J. Am. Chem. Soc. 116*, 6981−6982.
Diner, B. A., & Babcock, G. T. (1996) in *Advances in Photosynthesis* (Ort, D., & Yocum, C. F., Eds.) pp 213−247, Kluwer, Dordrecht, the Netherlands.
Doan, P. E., Fan, C., & Hoffman, B. M. (1994) *J. Am. Chem. Soc. 116*, 1033−1041.
El-Kabbani, O., Chang, C.-H., Tiede, D., Norris, J., & Schiffer, M. (1991) *Biochemistry 30*, 5361−5369.
Fajer, J., Davis, M. S., Brune, D. C., Spaulding, L. D., Borg, D. C., & Forman, A. (1977) *Brookhaven Symp. Biol. 28*, 74−105.
Fromme, P., Witt, H. T., Schubert, W.-D., Klukas, O., Saenger, W., & Krauss, N. (1996) *Biochim. Biophys. Acta 1275*, 76−83.
Golbeck, J. (1992) *Annu. Rev. Plant Physiol. Plant Mol. Biol*, *43*, 293−324.
Goldsmith, J. O., King, B., & Boxer, S. G. (1996) *Biochemistry, 35*, 2421−2428.
Hanson, L. K. (1990) in *Chlorophylls* (Scheer, H., Ed.) pp 1015−1042, CRC Press, Boca Raton, FL.
Käss, H., & Lubitz, W. (1996) *Chem. Phys. Lett, 251*, 193−203.
Käss, H., Bittersmann-Weidlich, E., Andreasson, L.-E., Bonigk, B., & Lubitz, W. (1995) *Chem. Phys, 194*, 419−432.
Kevan, L., & Kispert, L. D. (1976) in *Electron Spin Double Resonance Spectroscopy*, pp 2−57, John Wiley and Sons, New York.
Krauss, N., Hinrichs, W., Witt, I., Fromme, P., Pritzkow, W., Dauter, Z., Betzel, C., Wilson, K. S., Witt, H. T., & Saenger, W. (1993) *Nature 361*, 326−330.
Lendzian, F., Lubitz, W., Scheer, H., Hoff, A. J., Plato, M., Trankle, E., & Mobius, K. (1988) *Chem. Phys. Lett. 148*, 377−385.
Lendzian, F., Huber, M., Isaacson, R. A., Endeward, B., Plato, M., Bonigk, B., Mobius, K., Lubitz, W., & Feher, G. (1993) *Biochim. Biophys. Acta 1183*, 139−160.
Lin, C. P., Bowman, M. K., & Norris, J. R. (1985) *J. Magn. Reson. 65*, 369−374.
Lin, S., Murchison, H. A., Nagarajan, V., Parson, W. W., Williams, J. C., & Allen, J.P. (1994) *Proc. Natl. Acad. Sci. U.S.A. 91*, 10265−10269.
McCracken, J., Shin, D.-H., & Dye, J. L. (1992) *Appl. Magn. Reson. 3*, 30.
Mehring, M., & Freysoldt, F. (1980) *J. Phys. E: Sci. Instrum*. 13, 894−895.
Mims, W. B. (1972) *Phys. Rev. B 5*, 2409−2419.
Mims, W. B. (1984) *J. Magn. Reson. 59*, 291−306.
Mouesca, J.-M., Noodleman, L., Case, D. A., & Lamotte, B. (1995) *Inorg. Chem. 34*, 4347−4359.
O'Malley, P. J., & Babcock, G. T. (1984) *Proc. Natl. Acad. Sci. U.S.A. 81*, 1098−1101.
O'Malley, P. J., & Babcock, G. T. (1986) *J. Am. Chem. Soc. 108*, 3995−4001.
Petke, J. D., Maggiora, G. M., Shipman, L. L., & Christoffersen, R. E. (1980) *Photochem. Photobiol. 31*, 243−257.
Plato, M., Mobius, K., & Lubitz, W. (1990) in *Chlorophylls* (Scheer, H., Ed.) pp 1015−1042, CRC Press, Boca Raton, FL.
Rautter, J., Lendzian, F., Lubitz, W., Wang, S., & Allen, J. P. (1994) *Biochemistry 33*, 12077−12084.
Reddy, M. V. V. S., Lingam, K. V., & Gundu Rao, T. K. (1982) *J. Chem. Phys. 35*, 4398.
Rippke, R., DeRuelles, J., Waterbury, J. B., Herdman, M., & Starkier, R. Y. (1979) *J. Gen. Microbiol. 111*, 1−61.
Robert, B., & Moenne-Loccoz, P. (1990) in *Current Research in Photosynthesis* (Baltscheffsky, M., Ed.) Vol. 1, pp 65−68, Kluwer, Dordrecht, The Netherlands.
Schenck, C. C., Gaul, D., Steffen, M., Boxer, S. G., McDowell, L., Kirmaier, C., & Holten, D. (1990) in *Reaction Centers of Photosynthetic Bacteria: Feldafing II* (Michel-Beyerle, M. E., Ed.) pp 229−238, Springer Verlag, Berlin.
Tang, X.-S., Diner, B. A., Larsen, A. S., Gilchrist, M. L., Lorigan, G. A., & Britt, R. D. (1994a) *Proc. Natl. Acad. Sci. U.S.A. 91*, 704−708.
Tang, X.-S., & Diner, B. A. (1994b) *Biochemistry 33*, 4595−4603.
Zysmilich, M. G., & McDermott, A. E. (1994) *J. Am. Chem. Soc. 116*, 8362−8363.

BI961765F